A Study of the Veil Cells Around Normal, Diabetic, and Aged Cutaneous Microvessels

Irwin M. Braverman, M.D., Jane Sibley, B.A., and Agnes Keh-Yen, B.S., M.S.
Department of Dermatology, Yale University School of Medicine, New Haven, Connecticut, U.S.A.

The veil cells around normal, diabetic, and aged vessels were reconstructed in 3 dimensions by a computer graphics system from 120–140 serial ultrathin sections. The normal vessel was surrounded by a single layer of veil cells which had a wrinkled and pleated surface. The diabetic vessels were surrounded by 3–6 layers of cellular material produced by increased numbers of veil cells and their associated cytoplasmic sheets. The veil cells around aged vessels appeared to have the same length as young and diabetic veil cells but were underdeveloped in their lateral extensions so that they did not cover the vessel circumferentially as well as did the normal veil cells. Preliminary data suggest that young, diabetic, and aged veil cells have the same metabolic activity per unit area of cytoplasm and are of the same length. The abnormal thickness or thinness of the vascular wall of dermal microvessels appears to be related to the degree of development and numbers of veil cells around the vessels rather than any change in their basic metabolic activity from normal. *J Invest Dermatol 86:57–62, 1986*

The veil cells are flat fibroblast-like cells that surround all the dermal microvessels [1]. Unlike pericytes which are an integral component of the vascular wall and are enmeshed in the mural basement membrane material, the veil cells are totally external to the wall. The veil cell demarcates the vessel from the surrounding dermis and can be considered to be an adventitial cell. The veil cells are seen infrequently around the microvessels in the subcutaneous fat and it is not known whether they are present in significant numbers around microcirculatory vessels in other organs [2].

In previous studies we observed that the veil cells appeared to be larger and more numerous around the thickened vessels in sun-damaged skin, diabetic skin, and buttock skin of some aged individuals [3,4]. The vascular wall of these vessels is produced by a belt of basement membrane-like material in which are enmeshed small collagen fibrils. This belt of connective tissue is laid down on the periphery of the vascular wall and is intimately associated with the veil cells. Some aged persons have abnormally thin vascular walls and in these situations the veil cells are scant and appear underdeveloped [3].

The purpose of this paper is to describe the morphology and spatial relationships of the veil cells in normal, juvenile diabetic, and aged microvessels. In addition, preliminary data about the size and functional activity of the veil cells in these 3 clinical situations will be presented.

MATERIALS AND METHODS

Blocks of normal, juvenile diabetic, and aged buttock skin embedded in Spurr resin which demonstrated the characteristic features of normal, thickened, and thin vessels found in these 3 clinical situations were selected from previous studies [1,3,4]. A total of 120–140 serial ultrathin sections 80–90 nm in thickness were prepared for examination by electron microscopy (EM) and stained with uranyl acetate and lead citrate. A total of 120–140 serial 1-μm sections were made from the same blocks and stained with methylene blue-Azure II for study of veil cells by light microscopy. The specimens came from a 30-year-old normal man, a 32-year-old juvenile diabetic woman, and a 78-year-old nondiabetic man. Three vessels in each specimen were selected for study. In the EM studies each vessel was serially sectioned, examined on single-slotted Formvar-coated grids, and photographed. On the resulting prints, the endothelial cells, pericytes, periphery of the normal basement membrane material, and the abnormal belts of basement membrane material, the veil cells, and mast cells were each outlined and the profiles were traced onto transparent acetate sheets. Fiducial marks were made on the sheets by reference to tissue landmarks so that all the sections would be correctly aligned for the digitization process. The outlines on each sheet were traced on the digitizing pad thereby feeding the X, Y coordinates into the computer for eventual processing into 3-dimensional models. The design and function of the computer system is described in detail elsewhere [5]. In this paper, we present the relationships between the veil cells, the basement membrane material, and the vessel outline as well as the 3-dimensional images of individual veil cells. The veil cells were reconstructed as wire frame models in which the consecutive boundaries of the sections of each veil cell were connected to produce artistic renderings of the cells both as individual entities and in relation to the vessels. By using different colors for each element in the microvascular unit, the relationships among them could be more easily visualized.

The serial 1-μm sections (120–140 in number) were photographed. For each cross-sectioned vessel, the section levels at which a veil cell first appeared and then completely disappeared were determined. Thus, the number of consecutive sections in which a veil cell could be found, multiplied by the thickness of the section, determined the length of the veil cell parallel to the long axis of the vessel. Three entire veil cells were thus measured in the aged and diabetic specimens and 2 were measured in the normal young specimens. Other veil cells were present but either the beginning or the end of the cell was not included in the series of sections.

To assess the functional activity of the veil cells, autoradiography with tritiated proline and lysine was performed with dermal tissue slices from normal, juvenile diabetic, and aged buttock skin. The purpose of these experiments was to correlate amino acid uptake activity with the morphologic appearance of the veil cells by EM and to see whether the amino acids taken up and processed

Manuscript received April 1, 1985; accepted for publication July 23, 1985.
This work was supported by NIH grants AM 15739 and AG 03295.
Reprint requests to: Irwin M. Braverman, M.D., Department of Dermatology, Yale University School of Medicine, 333 Cedar Street, New Haven, Connecticut 06510.
Abbreviation:
EM: electron microscopy
MEM: minimal essential medium (Eagle)

by the cells could be found in the peripheral portion of the basement membrane of the normal vessel and in the abnormal connective tissue belt found around diabetic vessels.

Thin slices of fresh buttock dermis (prepared for 3-mm punch biopsies) were obtained from 3 young normal (29, 28, 30 years), 3 juvenile diabetic (25, 37, 42 years), and 3 aged (74, 78, 79 years) volunteers. The slices were incubated for 24, 48, and 72 h in α-MEM (Eagle's minimal essential medium), a chemically defined medium containing inorganic salts, glucose, pyruvate, lipoic acid, amino acids, vitamins, and ribo- and deoxyribonucleosides.

The best uptake and labeling occurred when 50 μCi of tritiated amino acid (sp act 40–50 Ci/mmol, New England Nuclear) was used in conjunction with the corresponding cold amino acid in a total concentration of 1–1.5 mg/liter in the medium. The ratio of cold to hot amino acid was approximately 33:1 by weight. The slices were incubated in 5 ml of α-MEM at 37°C for 24 h with 95% O_2 and 5% CO_2. After washing in cold α-MEM 3 times, the tissues were fixed in half-strength Karnovsky's fixative, washed in cacodylate buffer, postfixed in osmium tetroxide, passed through alcohols, and embedded in Spurr resin. Autoradiography was performed on 1-μm and ultrathin sections by coating with Kodak NTB-2 emulsion for light microscopy and Ilford L-4 emulsion for EM and exposing the sections for 4 weeks.

The 48- and 72-h incubations, in spite of medium changes at 24-h intervals with or without added pulses of tritiated amino acid, showed a moderate amount of cellular death. Therefore only the 24-h incubations which were uniformally morphologically viable were used for comparisons and measurements.

The lysine was associated with a much greater uptake and labeling than the proline. Because the silver grains from the lysine were too dense for accurate counting, the proline experiments were used for measurements. Twelve vessels were measured in each patient. The outlines of all veil cells around each vessel were traced on photographs, *uniformly* printed at the same magnification (× 5760), on the digitizing pad of the computer system. Our computer program calculates area from the measurement of perimeter by the trapezoidal rule function. The number of silver grains in each veil cell was counted, entered into the computer after each veil cell outline was traced, and the ratio of grains/cm^2 of veil cell was calculated for each individual veil cell profile. The "cm^2" value relates to the actual areas of the veil cells on the photographs that were printed at a uniform magnification of 5760 ×. The values on each patient were expressed as the mean ± SEM and the mean values between each of the 3 groups was tested for statistical significance by the Student's *t*-test.

These experiments were approved by the Human Investigation Committee at Yale University.

RESULTS

Figs 1–3 briefly illustrate the process of the 3-dimensional computer reconstruction used in this study. Fig 1 is a drawing of a typical serial cross-section of a normal vessel. The cells, pericytes, peripheral boundary of basement membrane, and veil cells are each traced on the digitizing pad and assigned a different color so that they can be distinguished from each other when they are eventually displayed. Fig 2 is a photograph of a printout of 30 consecutive sections of veil cells. Only the X, Y coordinates representing the veil cells have been drawn and the 30 serial outlines have been tilted 60° on the X-axis toward the viewer. Fig 3 is the drawing made from these 30 serial sections which represent portions of 4 veil cells. The adjacent points on consecutive sections have been joined together to produce this illustration. By comparing the original EM photographs with the computer printout, one can produce an accurate rendering of the veil cell including major cell surface contours.

Veil cells around normal vessels in young buttock skin are illustrated in Figs 4–6. Fig 4 shows in outline form the relationship

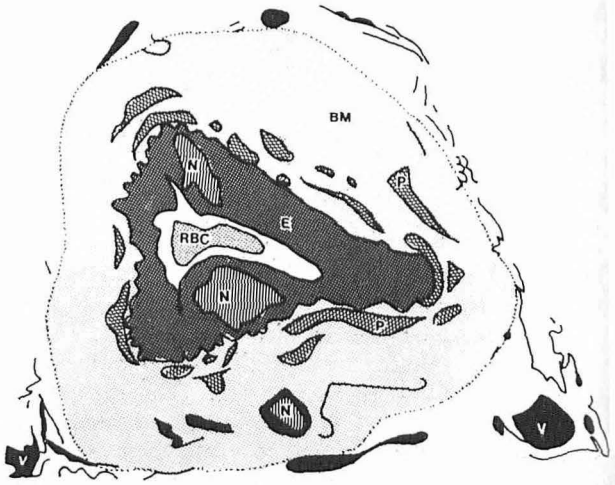

Figure 1. Drawing of typical ultrathin cross-section used in reconstructions. *V and solid black lines* = veil cell. *N* = nucleus. *E* = endothelial cell. *P* = pericyte. *RBC* = erythrocyte. *BM* = basement membrane of vascular wall.

between the veil cells (V), the outermost boundary of the normal basement membrane of the vascular wall (BM), and the endothelial cell outline (B). The veil cells almost completely surround the vessels just outside the periphery of the basement membrane material. However in some spots the cytoplasmic processes are in apposition to the basement membrane, and in others they may be present just within the outer boundary so that basement membrane material is present on both the ab- and adluminal sides of the veil cell. Fig 5, also in outline form and with the vessel and basement membrane layer removed, illustrates how the veil cells surround the vessel. They form a layer usually one cell layer thick but they overlap at their margins. The peripheral cytoplasm of some veil cells contained open areas that might represent spaces formed by a retiform cytoplasm. The individual veil cells had configurations. Some were flat with minimal wrinkling as they surrounded the vessel but the majority had a compressed, wrinkled, and pleated surface (Fig 6). When 2 vessels were adjacent to each other we observed a single veil cell with 3 cytoplasmic arms; two extended over a portion of each vessel and the third was present as a common sheet between them.

In aged skin where the vascular walls were thin, the veil cells were fewer in number and encircled the vascular wall much less extensively (Fig 7). The cells also had a less wrinkled and pleated

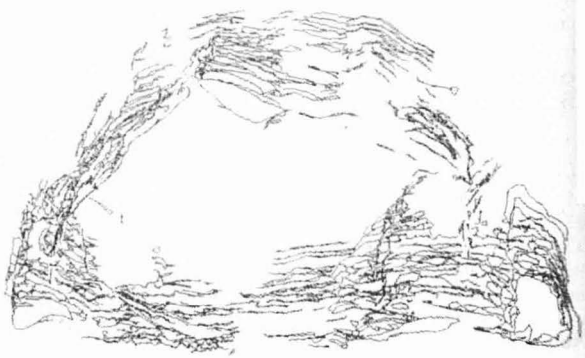

Figure 2. Computer printout of 30 serial veil cell outlines in form of wire frame model tilted 60° on X-axis toward viewer.

Figure 3. Drawing made from wire frame printout of veil cell outlines shown in Fig 2.

surface (Fig 8). Ultrastructurally the veil cells in aged skin contained fewer cellular organelles than the veil cells around normal or diabetic vessels, suggesting that they might be metabolically less active.

Fig 9 illustrates the typical appearance of a cross-section of a diabetic microvessel. The belt of connective tissue (NBM) that produces the thickened walls in diabetic vessels lies outside the normal basement membrane of the vascular wall (BM) and encompasses the veil cells to a great extent. The veil cells around diabetic vessels were present in increased numbers and formed 3–6 overlapping layers. Fig 10 shows the outlines of these overlapping cells in relation to the vascular wall. Fig 11 shows the surface contours of the veil cells. The vascular outline has been deleted from the reconstruction in Fig 11. The veil cells were smoother and less wrinkled and pleated than normal veil cells. Fig 12 is a computer-generated model illustrating how the veil cells surround the diabetic vessel. The lumen, normal basement membrane material, and the veil cells are shown in different colors. In contrast, the computer-generated model in Fig 13 shows these same relationships with the abnormal connective tissue belt included. The belt of abnormal connective tissue encases the veil cells almost completely. Portions of veil cells protrude through

Figure 5. Drawing made from wire frame printout of young veil cells. Vessel outline in Fig 4 had been removed. Simplified view of overlapping veil cells shown.

this blanket of material. Ultrastructurally the diabetic veil cells were indistinguishable from the veil cells surrounding normal vessels.

The shapes of the individual diabetic veil cells were different from those observed in normal and aged veil cells. Instead of being wrinkled and pleated as in normal cells, the diabetic veil cells had extensive, thin, broad cytoplasmic processes developing from the central nuclear portion of the cell. The diabetic veil cells had 2–4 of these broad cytoplasmic processes resembling wings. In some cells, the processes folded back on themselves so that they resembled a flattened "sigma" shape. Fig 14 shows an example of a veil cell with 4 "wings." The arrow indicates the concave portion that surrounds the vessel. Fig 15 is a schematic drawing of the veil cell shown in Fig 14 indicating its spatial configuration. Figs 16 and 17 illustrate 2 other conformations of

Figure 4. Drawing made from wire frame printout of young vessel. Endothelial cell outline (*B*) with its normal basement membrane (*BM*) surrounded by a normal complement of veil cells (*V*).

Figure 6. Drawing made from wire frame printout of young veil cells. Same as Fig 5 except surface contours of veil cells are shown.

Figure 7. Drawing made from wire frame printout of aged vessel. Endothelial outline (*B*) with its normal basement membrane (*BM*) surrounded by underdeveloped veil cells (*V*).

Figure 8. Drawing made from wire frame printout of aged vessel in Fig 7 with vessel outline removed and surface contours of underdeveloped veil cells illustrated.

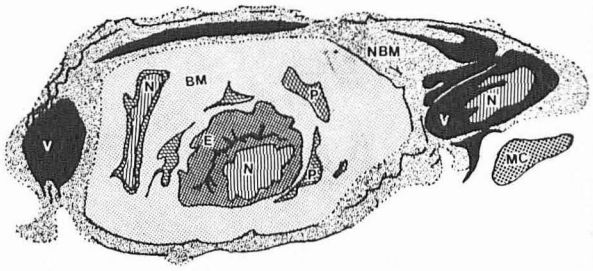

Figure 9. Drawing of typical section of diabetic vessel from which re constructions were made. Belt of abnormal basement membrane materia (*NBM*) surrounds normal basement membrane material (*BM*) of vascula wall and encases veil cells (*V*). *N* = nucleus, *E* = endothelial cell. *P* = pericyte. *MC* = mast cell.

diabetic veil cells. Since the EM serial sections represented a bloc of tissue 11–13 μm thick, only about half of individual veil cell could be reconstructed.

By light microscopy we were able to identify with certainty the beginnings and ends of 2–3 veil cells in the 120–140 1-μm serial sections of young, diabetic, and aged skin. Two norma veil cells extended for 33 μm along the length of the vessel; diabetic veil cells extended for 33–38 μm along the vessel; and aged veil cells ranged in length from 23–36 μm.

The results of the autoradiography experiments are shown in Table I. These specimens were obtained from each of the vol unteer groups: young, aged, and juvenile diabetics.

The differences in the values of silver grains/cm^2 between age and diabetic veil cells were not statistically significant. Althoug there was a borderline significant difference between young an aged veil cells ($p = 0.05$), this may be misleading because of th outlier value of 6.1 grains/cm^2 in young volunteer no. 2.

We did not observe a significant amount of label that wa unequivocally secreted into the basement membrane material o the vascular wall from the veil cells in the 24-, 48- or 72-h uptak studies.

DISCUSSION

The EM reconstructions of the veil cells were based on tissu serially sectioned over a distance of approximately 11–13 μm The light microscopic studies designed to determine the lengt of veil cells involved serial 1-μm sections over a distance of 120–14 μm. The sections chosen for these reconstructions exhibited th

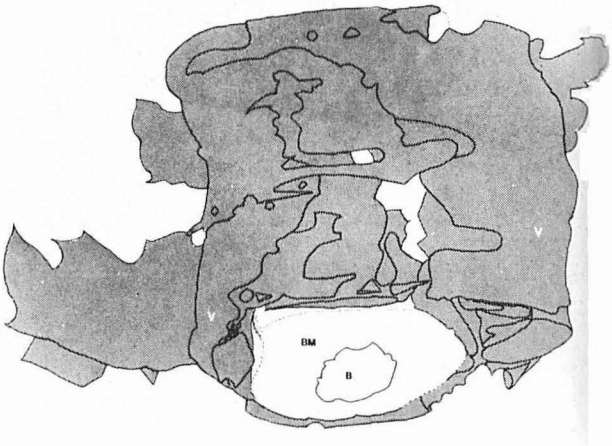

Figure 10. Drawing made from wire frame printout of diabetic ves Endothelial cell outline (*B*) with its normal basement membrane (*B* surrounded by increased numbers of enlarged overlapping veil cells.

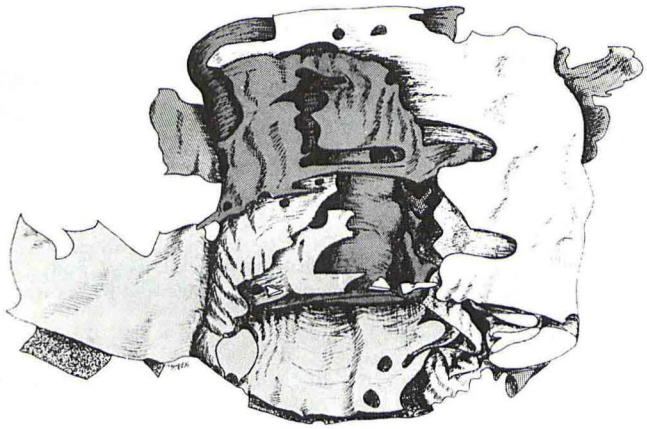

Figure 11. Drawing made from wire frame printout of diabetic vessel. Same model as in Fig 10 but surface contours of veil cells are shown. There is extensive overlapping of the cell bodies and cytoplasmic sheets of the veil cells.

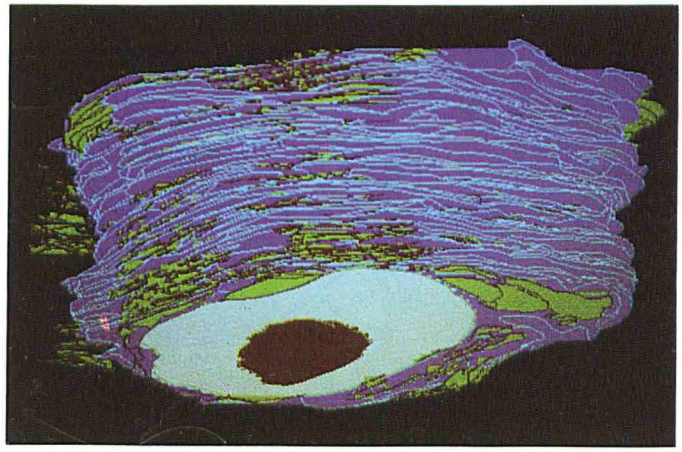

Figure 13. Computer-generated model of diabetic vessel shown in Fig 12. Belt of abnormal basement membrane material has been added to indicate relationship to veil cells. The abnormal material encases most of the veil cells. Endothelial cell outline = red. Normal basement membrane = white. Belt of abnormal basement membrane material = blue. Veil cell = green.

typical light and electron microscopic findings that we have observed in over 100 specimens representing the histologic findings in young normal, aged, and juvenile diabetic volunteers. Therefore we feel certain that the 3-dimensional relationships of the veil cells to the vessels and the individual morphology of partially reconstructed individual cells described above are a correct representation of the veil cells in these clinical settings. However more studies need to be performed to be certain that the preliminary findings related to functional activity and size of the veil cells are correct.

Our studies indicate that the veil cells around normal vessels are flat, wrinkled, and pleated, but those around diabetic vessels are increased in number and size and have extensive multiple cytoplasmic projections that radiate from the body in the form of "wings." The veil cells around the aged vessels appear to have the same length as their counterparts around the normal and diabetic vessels but lack circumferential development. Based upon the autoradiographic studies, it appears that all 3 categories of veil cells have the same metabolic activity per unit area, as defined by amino acid uptake. Therefore it appears that the increased deposition of connective tissue found around the diabetic vessels and the decreased amount of normal basement membrane around aged vessels are related to the number and cytoplasmic development of the veil cells per se rather than a difference in the metabolic activity of the different categories of veil cells. It would appear that the metabolic activity of veil cells per unit area as defined above may not decrease with age. The wrinkled and pleated surface of the normal veil cells may represent the cells' reserve to expand into broader sheets when it becomes necessary. The veil cells of the diabetic vessels had broad, relatively flat surfaces in addition to the 1 or 2 extra cytoplasmic sheets. These extra sheets as well as the way in which the sheets may fold back on themselves would provide an increased surface area for the synthesis and deposition of the connective tissue material deposited as a belt around diabetic vessels.

Although we have not yet specifically studied the thickened vessels in actinically damaged skin, the photosensitive porphyrias, lupus erythematosus, or other photosensitivity disorders by these reconstruction techniques, it is highly likely that the vascular wall thickening and prominent veil cells observed by light microscopy and EM in these conditions [6–9] would show the same 3-dimensional configurations.

We were unable to demonstrate the secretion of labeled material

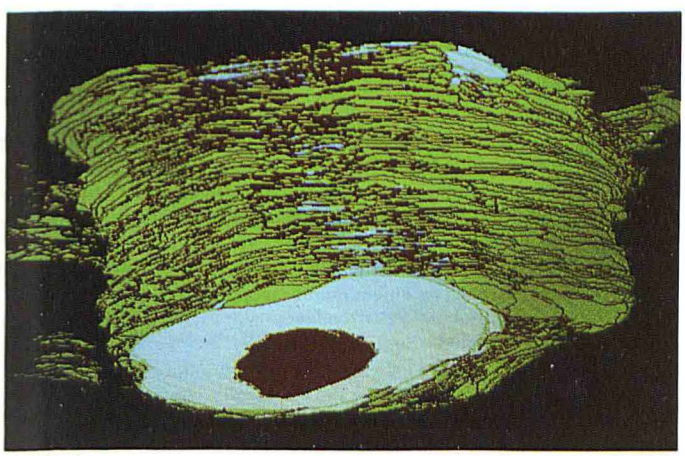

Figure 12. Computer-generated model of the diabetic vessel shown in Fig 10. Veil cells (green) shown in relation to endothelial cell outline (red) and normal basement membrane (white). Compare with Fig 13.

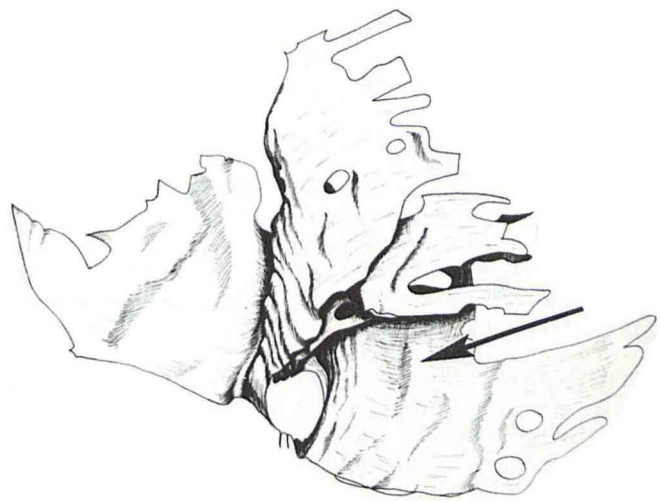

Figure 14. Drawing made from wire frame model of diabetic veil cell. Single veil cell with 4 cytoplasmic wings originating from central body of cell. *Arrow* indicates concavity which surrounds the vessel.

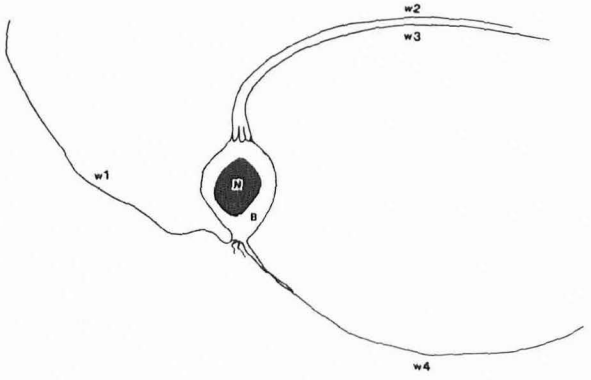

Figure 15. Schematic drawing of diabetic veil cell in Fig 14. *N* = nucleus. *B* = cell body. *W1–4* = Individual cytoplasmic "wings."

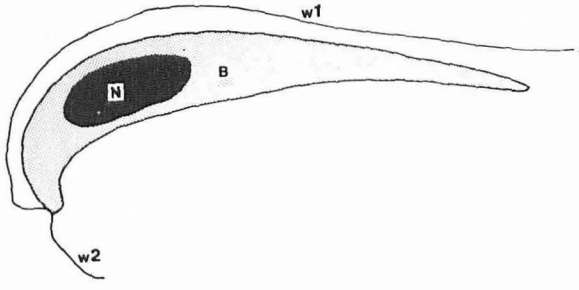

Figure 16. Schematic drawing of diabetic veil cell. *B* = Body, *N* = nucleus. *W1–2* indicate cytoplasmic "wings."

from the veil cell into the belt of abnormal connective tissue which would have provided a further link between these 2 elements. Pulse-chase experiments may be required to demonstrate this connection.

Light microscopic studies have emphasized that the vascular walls are excessively thickened in actinically damaged skin and in a variety of photosensitivity disorders [6–8]. The changes in diabetic skin are identical [4]. Peyrol et al [10] were similarly impressed by the relationship between vascular wall thickening and the prominence of the veil cells in diabetic skin. They demonstrated, using the immunoperoxidase technique, that the main component in the thickened basement membrane material of the vascular wall was the excessive and abnormal deposition of type IV collagen. Similarly in the various porphyrias exhibiting photosensitivity, the vessels are thickened by the deposition of type IV collagen and laminin [11]. In all likelihood the thickened vessels in actinically damaged skin are produced by the same mechanism. The nature of the protein deposition in the abnormally thin walls of aged vessels has not been studied. The similarity in the morphology of vascular wall thickening in actinic damage, photosensitization, diabetes mellitus, and in some aged-nondiabetic patients suggests that the veil cell response may be a nonspecific one to a variety of unrelated stimuli.

Further studies on the metabolic activity of the veil cells and their size are needed to substantiate our hypothesis that it is the number and development of veil cells that are related to vascular wall thickening rather than difference in metabolic activity between veil cells of young, diabetic, and aged individuals.

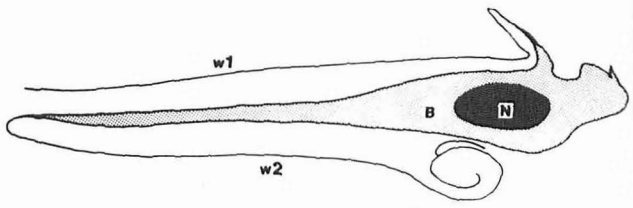

Figure 17. Schematic drawing of diabetic veil cell. *B* = Body, *N* = nucleus. *W1 and W2* show how cytoplasmic wings fold back on themselves.

Table I. Silver Grains Per cm^2 of Veil Cells ± SEM

Volunteer	No. 1	No. 2	No. 3
Young normal	2.6 ± .18	6.1 ± .72	3.6 ± .22
Juvenile diabetic	3.9 ± .69	2.9 ± .32	3.4 ± .46
Aged nondiabetic	3.4 ± .52	2.4 ± .19	3.1 ± .72
Young vs aged		$p = 0.05$	
Young vs diabetic		$p = 0.14$	
Diabetic vs aged		$p = 0.22$	

The color illustrations were provided through the generosity of Miles Pharmaceuticals Division of Miles Laboratories, Inc., West Haven, Connecticut.

REFERENCES

1. Yen A, Braverman IM: Ultrastructure of the human dermal microcirculation: the horizontal plexus of the papillary dermis. J Invest Dermatol 66:131–142, 1976
2. Braverman IM, Keh-Yen A: Ultrastructure of the human dermal and subcutaneous fat. J Invest Dermatol 77:297–304, 1981
3. Braverman IM, Fonferko E: Studies in cutaneous aging: II. The microvasculature. J Invest Dermatol 78:444–448, 1982
4. Braverman IM, Keh-Yen A: Ultrastructural abnormalities of the microvascular and elastic fibers in the skin of juvenile diabetics. J Invest Dermatol 82:1–4, 1984
5. Braverman MS, Braverman IM: Three dimensional reconstructions of objects from serial sections using a microcomputer graphics system. J Invest Dermatol, *in press*, 1986.
6. Epstein JH, Tuffanelli DL, Epstein WK: Cutaneous changes in the porphyrias. Arch Dermatol 107:689–698, 1973
7. Hashimoto K, Klingmuller G, Rodermund OE: Hyalinosis cutis et mucosae. An electron microscopic study. Acta Derm Venereol (Stockh) 52:179–195, 1972
8. Bauer EA, Santa-Cruz DJ, Eisen AZ: Lipoid proteinosis: in vivo and in vitro evidence for a lysosomal storage disease. J Invest Dermatol 76:119–125, 1981
9. Kumakiri M, Hashimoto K, Willis I: Biologic changes due to long wave ultraviolet irradiation on human skin: ultrastructural study. J Invest Dermatol 69:392–400, 1977
10. Peyrol S, Hugues B, Grimand JA, Mornex R: Collagen heterogeneity of thickened basement membranes of human diabetic dermis. Tissue immunolabeling of collagen types I, III and IV by light and electron microscopy. Cell Mol Biol 30:43–57, 1984
11. Wick G, Hönigsmann H, Timpl R: Immunofluorescence demonstration of type IV collagen and a noncollagenous glycoprotein in thickened vascular basal membranes in protoporphyria. J Invest Dermatol 73:335–338, 1979